WILEY | Hindawi

Research Article

Mechanism and Structural Parameter Optimization Method of Linear Energy-Gathering Cutting Device for Towering Steel Structures Based on Computational Intelligence

Xiaoguang Zhou (iD)

School of Mechanics and Civil Engineering, China University of Mining and Technology-Beijing, Beijing 100000, China

Correspondence should be addressed to Xiaoguang Zhou; bqd1800604041@student.cumtb.edu.cn

In the process of urban expansion, due to the advantages of high strength and light weight of steel frame structure, it has replaced concrete structure, and the construction technology of towering steel structure has been paid attention to by the construction industry. With the passage of time, steel structure also needs to be removed. In order to adapt to the efficient cutting of steel frame structures, this paper studies a new technology of linear energy-gathering cutting of towering steel structures based on computational intelligence methods. The research results of the article show the following: (1) The greater the penetration depth, the greater the setting of the cutter parameters. According to the experimental results, the designed towering steel structure cutter can smoothly cut more than 10 kinds of towering steel structure materials. It can be seen that the calculation results are basically accurate and the relative error of the calculation remains around 6%. (2) In the computational intelligent analysis method, the total stress is larger than that of the other two analysis methods, and the support stability force is slightly lower than the stress ratio of the direct analysis method, and the computational intelligent analysis method accounts for the largest axial force. (3) The cutting depth and slit width are different at different cutting speeds. When the cutting speed is 8, the cutting depth reaches the maximum value of 1.2300, and 90% of the experimental data errors can be controlled within 10%.

1. Introduction

The development of industrial technology has also substituted steel frame materials into industrial buildings. Although the steel frame structure in my country has not yet become common, the success of the bird's nest has laid a good foundation for the steel frame structure in my country. Buildings have also won the favor of many construction workers. Frame structure buildings have many advantages such as environmental protection and earthquake resistance. These advantages make steel frame structures continue to develop in my country's construction industry. Due to the stability of the steel frame structure, the traditional building cutting method can no longer meet the needs of the steel frame structure removal, so the steel frame structure removal technology has become a new research topic in the construction industry. This paper provides an overview of the modeling approach and its application in the design of a 10 kW proto-type wave energy conversion system tested on the open ocean in the fall of 2008 [1]. This paper proposes a segmented permanent magnet linear generator structure specially designed for wave energy converters [2]. In this paper, combined with the splicing characteristics of GRC materials, the steel structure + GRC modular assembly process is adopted to solve the construction scheme of the entire tower group system safely, economically, and efficiently [3]. In this study, the downwind and crosswind vibration characteristics of such equipment with flow limiters were investigated experimentally and numerically, and this work has important guiding significance for the design of frame-type towering process equipment [4]. In order to study the dynamic characteristics of composite towering structures under different working conditions, simulation research was carried out under various working conditions with different lifting ranges, different lifting ratios and payload swing directions [5]. This paper briefly

introduces the working principle of active vibration control and reviews the research progress of this technology at home and abroad in recent years, including control theory and algorithm, experimental research, and practical application [6]. The article compares the evaluation of wind loads in the 2012 Building Structural Load Regulations and the 2004 Steel Tower Mast Structural Design Regulations and illustrates the effects of the two versions on wind loads through calculation examples [7]. This project adopts the construction technology of internal and external dual control, subsection measurement, and electric climbing formwork rectification and has achieved good results in the transformation of the main shaft of the towering structure and the control of the verticality [8]. This paper proposes a cable mass damper system for controlling the vibration of towering structures during strong winds and earthquakes [9]. This paper describes the observation method and observation process of the sunlight deformation of the towering reinforced concrete structure and initially obtained the basic law of the sunlight deformation of the towering reinforced concrete structure [10]. This paper firstly presents a comprehensive and systematic introduction and review of the research progress of wind-induced response and wind-induced vibration control and then proposes some major issues that require further research [11]. Based on a typical example, this paper analyzes the key points and methods of the safety test and identification of the ground-type billboard structure, applies the proprietary software to carry out numerical simulation analysis of the wind load, and finally draws a conclusion based on the test results [12]. In this paper, a TDMA scheduling algorithm for general k-hop networks is proposed, and a detailed performance analysis of the algorithm is performed [13]. The article outlines the different operating principles and various linear generator types, analyzes the advantages and disadvantages, and presents a complete scheme that collects the most important characteristics [14]. This paper introduces the installation method of the towering steel pins on the roof of the PDOC office building in Khartoum, Sudan, and studies the structural response of conventional and diagonal grid buildings to evaluate the structural advantages of the diagonal grid system [15].

2. Analysis of Towering Steel Structure Line and Cutting Device

2.1. Problems Existing in the Design of Towering Steel Structures.
Due to the characteristics of fast construction speed and easy transformation during use, steel structures have been increasingly valued by industrial builders in recent years. Due to the great difference, if the simple calculation mode of ordinary civil buildings is simply applied, it will inevitably lead to deviations in the calculation. The main material used in the construction of steel structures is noncombustible steel, and the heat resistance of steel is not good. Under high heat conditions, steel structures are prone to rupture. If a fire is caused, it will seriously affect the safety, cause damage to the steel structure and cause huge safety hazards. Therefore, fire protection should also be fully con-

sidered in the design of steel structures. Another fatal flaw of the steel structure material is the unstable physical and chemical properties. The steel structure material exposed to the outdoor natural environment for a long time will suffer from rainwater and air pollution, which will not only harm the beauty of the steel structure but also the overall appearance of the steel structure is jeopardized, so the corrosion resistance of the steel structure should also be fully considered when designing the steel structure. Noise is a problem that is easy to ignore in today's residential construction, and it is also a problem that is not easy to deal with. Effective noise reduction has always been a key issue in the construction field. Buildings with various functions have different requirements for sound insulation. For buildings that need to improve sound insulation, relevant designers have to make targeted adjustments to the functions of the building.

2.2. Linear Energy-Gathering Cutting Device.
With the expiration of the service life of urban construction and steel structure facilities such as railway stations, factories, power line towers, TV, or communication towers, the demand for industrial technological transformation has increased significantly, and more and more steel structure buildings have to be demolished by enterprises. With the advancement of science and technology and the development of material technology, the application of steel structures in various facilities in cities and factories will become more and more extensive in the future, and the proportion of steel structures in building structures will become larger and larger. Over time, these steel structures may also be demolished. The linear concentrator is a rod-shaped charge structure, which is composed of three parts: high-performance explosive, metal charge cover, and shell. The basic principle of the linear concentrator cutting equipment to form a metal beam to cut metal is: After one end or center of the linear shaped charge explodes, the detonation wave propagates along the length of the charge on the one hand and moves downward in the direction. On the other hand, the action of the charge cover acts on the charge cover type with a pressure of up to tens of millions of Pa. The metal cover of the medicine type is crushed under the action of this extremely high pressure, moves inward at high speed, and collides with the symmetry plane. Upon collision, the metal near the inner wall of the drug-type cap forms on the symmetry plane, and the thin blade-like jet at the bottom of the drug moves at high speed, which is called "energy-gathering blade."

3. Setting of Linear Energy-Gathering Cutting Device for Towering Steel Structure

3.1. Mechanism of Linear Energy-Gathering Cutting Device.
The microelement crushing speed formula of the cutter is as follows[16]:

$$V_{oi} = \frac{D}{2} \sqrt{A(\varphi_i)\mu_i \left| 1 - \left(\frac{B}{b+B} \right)^2 \right|}, \tag{1}$$

$$\mu_i = \frac{\rho_e B}{\rho_j b}, \tag{2}$$

$$B = \left(LL - \frac{x}{\cos a}\right) tg\frac{a}{2}. \tag{3}$$

Among them, V_{oi} is the crushing speed of the cover cell, D_e is the detonation speed of the charge, μ_i is the ratio of the effective charge on each cell to the mass of the cover cell, ρ_e, ρ_j is the density of the charge and cover material, respectively, and B is the cover cell of the upper effective dose thickness, LL is the length of the cover bus, b is the thickness of the cover element, and $A(\varphi_i)$ is the detonation wave direction coefficient.

The influence on the explosion pressure can be calculated by the empirical formula [17]:

$$A(\varphi_i) = 1 + \frac{37}{27} \cos^2\varphi_i, \tag{4}$$

$$\varphi_i = 90° - \left(a - tg^{-1}\frac{xtga}{x+s}\right). \tag{5}$$

Among them, φ_i is the incident angle of the detonation wave reaching a certain microelement, a is the half of the top angle of the wedge-shaped cover, s is the distance from the detonation center to the top of the cover, and x is the coordinate origin of the cover vertex, and the abscissa value of each microelement of the cover.

Deformation angle calculation formula is as follows [18]:

$$\delta_i = \sin^{-1}\left(\frac{V_{0i}}{2D} \sin \varphi_i\right). \tag{6}$$

Jet microelement velocity is

$$V_{ji} = \frac{V_{0i}}{\sin(\beta_i/2)} \cos\left[(a + \delta_i) - \frac{\beta_i}{2}\right]. \tag{7}$$

The initial length of the jet element is as follows [19]:

$$L_{0i} = L_0\left[\frac{V_{ja} \sin \beta_i}{V_{0b} \cos(a+\delta_i)} - \frac{\cos[\beta_i - (a+\delta_i)]}{\cos(a+\delta_i)}\right]. \tag{8}$$

Effective length of jet microelement before penetration is

$$L_i = \frac{H - \varepsilon i + \sum L_i}{V_{j1}}\left(V_{j1} - V_{j2}\right) + L_{0i}. \tag{9}$$

Penetration depth calculation formula is as follows [20]:

$$L = ut = \frac{1}{V_j/u - 1}. \tag{10}$$

TABLE 1: Relationship between penetration depth and cutter parameters.

Serial number	L/mm	k/mm	b/mm	d/mm	G/mm	H/mm
1	8	0.981	0.8	7.80	11.70	7.80
2	9	0.981	0.8	8.55	12.825	8.55
3	10	0.981	0.8	9.25	13.875	9.25
4	11	0.981	0.8	10.00	15.00	10.00
5	12	0.981	0.8	10.70	16.05	10.70
6	13	0.905	1.0	10.45	15.675	10.45
7	14	0.905	1.0	11.00	16.50	11.00
8	15	0.905	1.0	11.60	17.40	11.60
9	16	0.905	1.0	12.25	18.375	12.25
10	17	0.905	1.0	12.85	19.275	12.85

According to the experiment, the following relationship can be obtained:

$$\frac{V_j}{u} = 1 + \sqrt{\frac{\rho_t}{\rho_j}}(V_j \geq 2.6V_k), \tag{11}$$

$$\frac{V_j}{u} = k\left(\left(1 + \sqrt{\frac{\rho_t}{\rho_j}}\right)\Big/\left(\sqrt{1 - \left(\frac{V_k}{V_j}\right)^2}\right)\right)(V_k \leq V_j \leq 2.6V_k). \tag{12}$$

The penetration depth calculation formula is as follows [21]:

$$L_i = L_i\left[\left(\left(k\left(1 + \sqrt{\frac{\rho_t}{\rho_j}}\right)\right)\Big/\left(\sqrt{1 - \left(\frac{V_k}{V_j}\right)}\right)\right) - 1\right]^{-1}. \tag{13}$$

3.2. Analysis of Towering Steel Structures.

The commonly used TLCD is mostly aimed at high-rise buildings, and its shape is U-shaped. Because the bottom pipe is connected and straight, it is not in harmony with the shape of the towering steel structure, so it is not suitable for direct use. Considering that the section of towering steel structure is mostly circular or nearly circular (such as octagon), two small TLCDs can be set in the direction of structure movement, and the other two are set in the direction of vertical structure movement.

From the dynamic balance of the liquid column, a single TLCD dynamic equation can be obtained [22]:

$$\ddot{w} + 2\bar{\zeta}_L\omega_L\dot{w} + \omega_L^2 w = -\left(\frac{B}{L}\right)\ddot{y}_k, \tag{14}$$
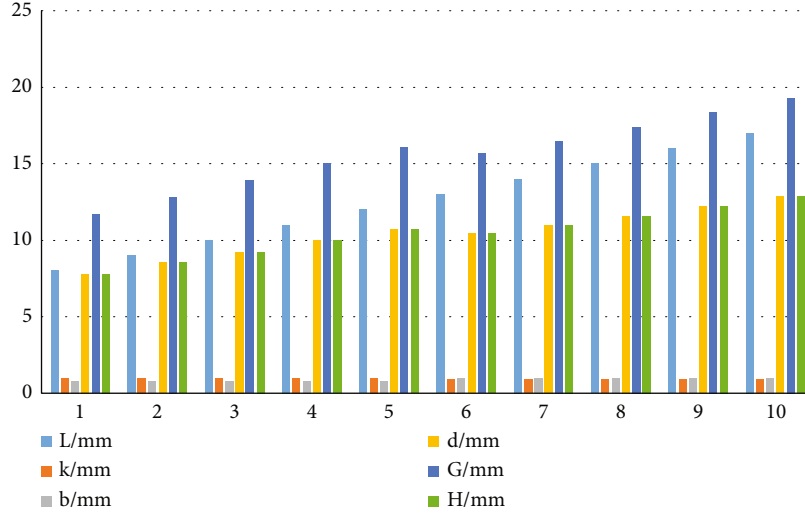
in

$$\omega_L = \sqrt{\frac{2g}{L}}, \tag{15}$$

FIGURE 1: Statistics of penetration depth and cutter parameters.

$$\bar{\zeta}_L = \sqrt{\frac{1}{(2gL)}} \zeta_L \frac{|\dot{w}(t)|}{4}. \tag{16}$$

The control force acting on the structural nodes is as follows [23]:

$$F_{TLCD} = -(\rho AB\ddot{w}(t) + \rho AL\ddot{y}_k). \tag{17}$$

The equation of motion of the structural system is as follows [24]:

$$[M]\{\ddot{y}(t)\} + [C]\{\dot{y}(t)\} + [K]\{y(t)\} = \{P(t)\}. \tag{18}$$

Model of the architecture after installing the ring TLCD is

$$[M]\{\ddot{y}(t)\} + [C]\{\dot{y}(t)\} + [K]\{y(t)\} = \{P(t)\} - [H]\{F_{TLCD}(t)\}. \tag{19}$$

Engineering satisfaction is

$$S_k(x) = \frac{1}{1 + \exp\left(((a(f_k(x)))/(f_{k0} - b))\right)}. \tag{20}$$

Compound satisfaction is as follows [25]:

$$S(x) = \sum_{k=1}^{n} w_k S_k(x). \tag{21}$$

4. Simulation Experiments

4.1. Calculation of Cutter Parameters. Because the structure of towering steel is complex, and the quality and hardness are not uniform, in order to design the cutter parameters for the cutting effect, the experiment calculates the cutter parameters according to the calculation method of cutter depth. It can be known from theory and practice that the

taper angle 2a is 80-90. The penetration depth is the best, generally 90 for the convenience of processing. $G = 1.5d$ is the optimal charge height, and further increase does not contribute much to the penetration depth. When the explosion height is $H = d$, it is the best explosion height. When the metal charge-shaped thick cover is $b = 0.05 - 0.08d$, the cutting effect. Therefore, it can be seen that when the value of b is determined, the penetration depth L and the bottom width d have a one-to-one correspondence. Therefore, the cutter with the designed penetration depth can be obtained according to the reverse order of the cutter penetration depth calculation method. The parameters of the cutter under the penetration depth of 8-17 mm are calculated in the experiment, and the penetration depth is sorted by serial number 1-10. The obtained cutter parameters of the penetration depth are shown in Table 1.

According to the experimental data in Figure 1, the greater the penetration depth, the greater the setting of the cutter parameters. When the cutting depth is 8 mm, the parameters of the cutter parameters are designed to be 7.8 mm, 11.70 mm, and 7.80 mm, respectively. When the depth is increased to 17 mm, the parameters of the cutter parameters are designed to be 12.85 mm, 19.275 mm, and 12.85 mm, respectively. Using the experimental calculation results, a towering steel structure cutter was designed, and more than 10 kinds of towering steel structure materials were successfully cut. It can be seen that the calculation results are basically accurate. In order to test the accuracy of the calculation method, the experiment also compares the penetration depth test value with the theoretical value. The calculation results are shown in Table 2 and Figure 2.

According to the experimental data in the table, we can conclude that the relative error of the calculation is kept at about 6%, the minimum relative error is 0.18%, and the maximum is 6.45. Relatively speaking, the larger the average penetration depth, the smaller the relative difference. When the penetration depth is 28.3 mm, the relative difference is only 0.67%, and when the penetration depth is 8.5, the relative difference is 2.52%.

TABLE 2: Penetration depth test and theoretical calculation value.

| Serial number	Cutter bottom width	Cover thickness	Fried high	Effective number of shots	Average penetration depth	L/d	k	Calculated value/mm	Relative difference/%
1	8	0.8	8	12	8.5	1.06	0.98	8.29	2.52
2	10	0.8	10	15	11.0	1.10	0.98	11.02	0.18
3	13	0.8	11	3	11.0	0.85	0.98	10.29	6.45
4	13	1.0	11	3	12.3	0.95	0.90	11.57	5.93
5	15	0.8	15	9	17.7	1.18	0.98	17.97	4.76
6	17	0.8	15	4	18.5	1.09	0.98	19.38	1.53
7	17	1.0	15	3	16.5	0.97	0.90	16.49	0.06
8	20	0.8	10	9	23.2	1.16	1.00	23.86	2.84
9	25	0.8	25	9	25.7	1.03	1.10	25.12	2.26
10	30	0.8	30	9	28.3	0.94	1.15	28.11	0.67
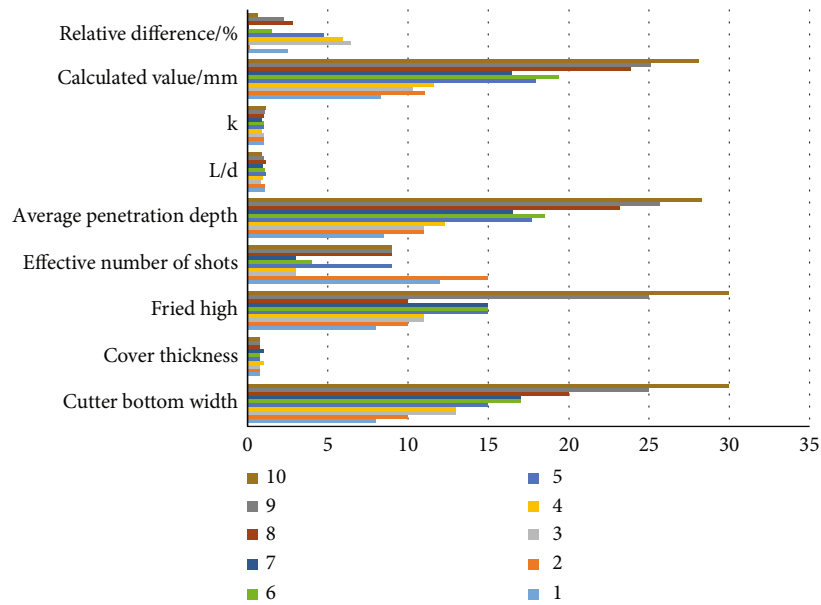
FIGURE 2: Penetration depth test and theoretical calculation value statistics.

4.2. Comparative Analysis of Tower Top Displacement.

The towering steel structure is a self-supporting structure. Three different analysis methods are used in the experiment. The modeling calculation and comparative analysis of a towering steel structure tower are carried out, and the stable stress ratio at different positions of the tower is analyzed. The tower top displacements calculated by the three calculation methods all meet the requirements of the Design Standards for Tall Structures, and the influence of the overall geometric defects of the tower structure on the horizontal displacement of the steel frame can be ignored. The tower displacement and corner column reaction force calculated by the three methods are shown in Tables 3 and 4.

The first-order analysis method considers the influence of the first-order effect on the internal force and deformation of the structure. Under the action of the load, the structure will produce a certain deformation, which will cause additional internal force in the structure, and the additional internal force will cause further additional deformation of

TABLE 3: Tower top displacement.

Tower top displacement (direction)	Displacement value (mm)	Horizontal displacement angle
Computational intelligence analysis	143	1/687
Direct analysis	143	1/687
First-order analysis	131.7	1/745

TABLE 4: Reaction force of a corner column at the bottom of the tower.

Tower bottom prism reaction force	F_x	F_y	F_z
Computational intelligence analysis	248.7	7.9	2529.74
Direct analysis	248.3	8.07	2546.02
First-order analysis	248.3	8.07	2546.02

TABLE 5: Stability ratio of a certain corner column of the tower.

Tower bottom corner column reaction force	Total stress ratio	Axial force ratio	Main bending moment ratio	Secondary bending moment ratio
Computational intelligence analysis	0.529	0.271	0.202	0.048
Direct analysis	0.526	0.273	0.206	0.048
First-order analysis	0.541	0.249	0.244	0.048

TABLE 6: Stable stress ratio of a certain support of the tower.

Tower bottom corner column reaction force	Total stress ratio	Axial force ratio	Main bending moment ratio	Secondary bending moment ratio
Computational intelligence analysis	0.554	0.579	0.084	0.001
Direct analysis	0.599	0.472	0.172	0.001
First-order analysis	0.343	0.151	0.193	0.007

the structure, and this additional deformation will cause a certain additional internal force in the structure, so the action is repeated until the additional effect produced is small. At this time, the relationship between deformation and load is nonlinear. According to the relevant provisions of the "Standards for Design of Steel Structures," the first-order analysis should consider the influence of the initial geometric defects of the overall structure. The first-order analysis method only considers the effect of the horizontal displacement of the structure on the vertical force, and does not consider the effect of the deflection (initial bending) of the member on the axial force. In fact, there are certain defects in the production, processing, transportation and welding of rods. In order to make up for this effect, the "Standards for Design of Steel Structures" provides a direct analysis method, which is a further improvement of the first-order analysis method. The calculation results of the three different methods are shown in Tables 5 and 6.

From the data in Figure 3, it can be seen that when the diagonal column is less than 49 meters, the direct analysis method and the first-order analysis method are used, and the influence of the stable stress ratio is not much different. The total stress ratio of the direct analysis method is 0.526, and the first-order analysis method is 0.541, the calculation intelligence analysis method is adopted, the total stress is larger than the total stress of the other two analysis methods, the total stress ratio is 0.529, and the proportion of the secondary bending moment of the three analysis methods is consistent; Axial force adopts computational intelligence analysis method. The proportion of the axial force and the proportion of the main bending axis are the smallest, which are 0.271 and 0.202, respectively. The proportion of the axial force and the main bending axis of the first-order analysis method is the largest, and the maximum values are 0.249 and 0.244, respectively. When the diagonal column is in the interval of 70 meters to 77 meters, the difference between the direct analysis method and the first-order analysis method is more than 10%, and the error of the computational intelligence analysis method is small. In general, the computational intelligence method is generally controllable.
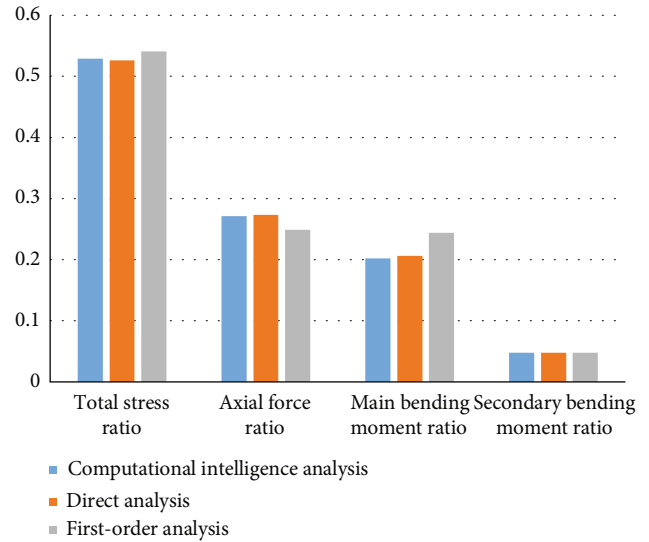

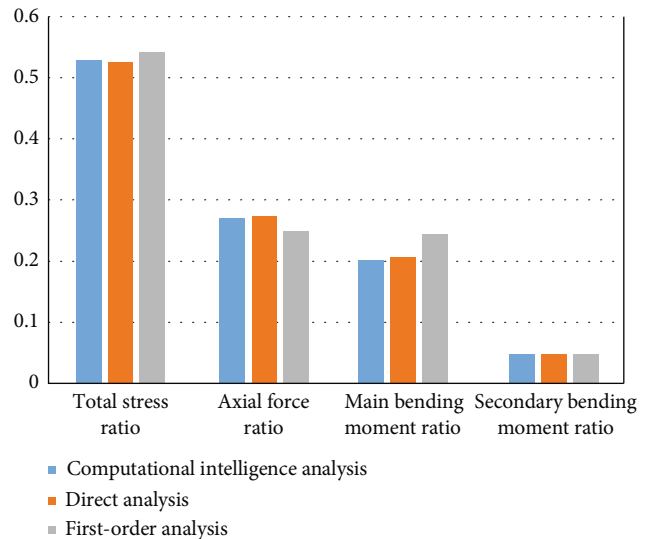FIGURE 3: Statistics of corner column stability force ratio.

FIGURE 4: Statistics of support stability stress ratio.

TABLE 7: Error analysis of mathematical model based on computational intelligence.

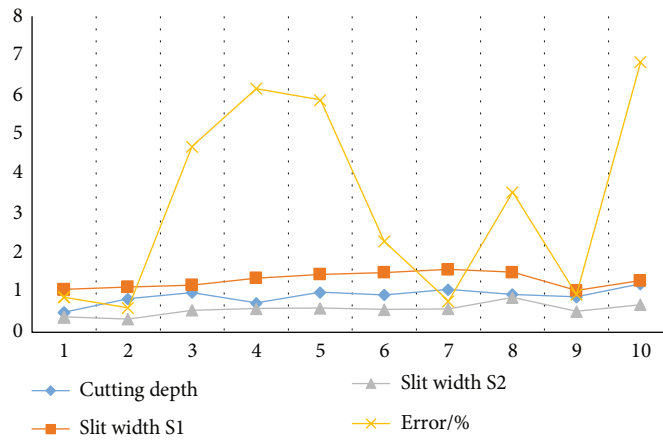| Test points	Cutting speed	Cutting depth	Slit width S1	Slit width S2	Test value	Calculated	Error/%
1	10.0	0.5090	1.0880	0.3892	200.00	201.77	0.89
2	10.0	0.8520	1.1530	0.3354	300.00	298.15	0.62
3	10.0	1.0100	1.2000	0.5594	400.00	418.84	4.71
4	15.0	0.7420	1.3740	0.6000	500.00	469.09	6.18
5	12.0	1.0130	1.4700	0.6137	500.00	529.45	5.89
6	15.0	0.9500	1.5190	0.5791	600.00	586.11	2.31
7	13.0	1.0880	1.5960	0.5953	600.00	604.72	0.79
8	13.0	0.9610	1.5230	0.8842	600.00	621.32	3.55
9	8.0	0.8960	1.0610	0.5280	300.00	302.87	0.96
10	8.0	1.2300	1.3100	0.7000	500.00	465.74	6.85

FIGURE 5: Statistics chart.

TABLE 8: Error analysis of mathematical model of cutting speed.

Test points	Power	Cutting depth	Slit width S1	Slit width S2	Test value	Calculated	Error/%
1	200.0	0.5090	1.0880	0.3892	10.00	10.28	2.77
2	300.0	0.8520	1.1530	0.3354	10.00	10.00	0.05
3	400.0	1.0100	1.2000	0.5594	10.00	9.29	7.13
4	500.0	0.7420	1.3740	0.6000	15.00	15.42	2.82
5	500.0	1.0130	1.4700	0.6137	12.00	11.52	4.03
6	600.0	0.9500	1.5190	0.5791	15.00	15.04	0.24
7	600.0	1.0880	1.5960	0.5953	13.00	13.20	1.52
8	600.0	0.9610	1.5230	0.8842	13.00	12.61	2.96
9	300.0	0.8960	1.0610	0.5280	8.00	7.81	1.65
10	500.0	1.2300	1.3100	0.7000	8.00	8.91	11.33

As shown in Figure 4, it can be concluded that when the direct analysis method and the first-order analysis method are used, the calculation results of the support stability stress ratio have little effect. When the calculation intelligent analysis method is used, the total stress ratio adopts the stress ratio of the direct analysis method. The ratio of axial force is the largest, the maximum value is 0.579, the first-order analysis method is the smallest, and the minimum value is 0.193. The ratio of the secondary moment of the intelligent analysis method and the direct analysis method is calculated to be 0.007, and the ratio of the secondary moment of the order analysis method is calculated to be 0.007..

4.3. Determination of Cutting Speed. Appropriate cutting speed is very important for the experiment. If the cutting speed is small, it will cause the light speed to stay in the same position for a long time, which will cause cracks or scorch on the cut surface; if the cutting speed is high, it will not work
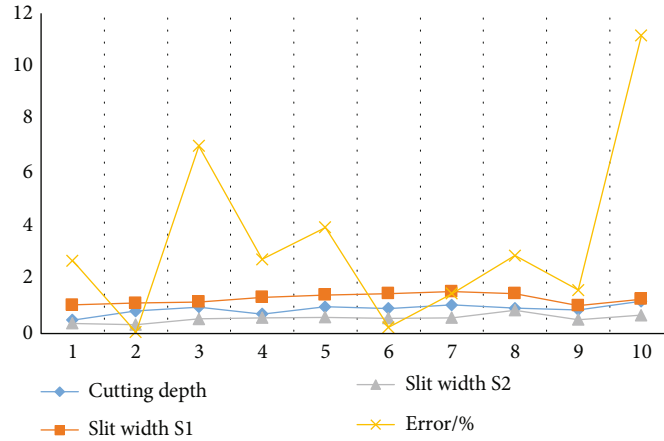
Figure 6: Error analysis of mathematical model.

properly. To cut off the workpiece, in order to determine the cutting speed of the linear energy-gathering cutting device, the cutting depth and kerf width of different cutting speeds were calculated in the experiment. The statistical results are shown in Table 7.

From the data in Figure 5, it can be concluded that the cutting depth and slit width are different at different cutting speeds. When the cutting speed is 8, the cutting depth reaches the maximum value of 1.2300, and the two slit widths are 1.3100 and 0.7000, respectively., the relative error value is high; when the cutting speed is 10, the error value is the smallest, the minimum value is 0.62%, the cutting depth at this time is 0.8520, and the two slit widths are 1.1530 and 0.3354, respectively. The error statistics of the experimental data are shown in Table 8.

As well as the data in Figure 6, we can conclude that the error value is generally small, 90% of the error can be controlled within 10%, the maximum error is 11.33%, the cutting depth at this time is 1.2300, and the minimum error is 005. The cutting depth is 0.8520, indicating that the cutting device can meet the actual production needs.

5. Conclusion

The use of linear energy harvesting cutting technology to demolish large steel structures is a brand-new application field in controlled blasting work. This technology is applied to the analysis, research, and successful training of steel structure demolition bridges and steel mill workshop demolition. The following conclusions can be drawn. The use of linear shearing technology to achieve rapid and safe demolition of large steel structures and the use of linear energy recovery cutting for steel structure demolition have obvious economic and social benefits, so it is welcomed. The combination of computer numerical simulation and field measurement provides a theoretical basis for the formulation and implementation of detonation technical solutions for steel structures. It is necessary to take supporting measures such as pretreatment, classification and delayed blasting, noise reduction, and shock absorption. The beneficial research on the application technology of linear cutting technology

in the demolition of steel bridges and steel structures provides a technical approach for the popularization and application of this technology in the demolition of large and complex steel structures and also provides a similar technical structure. In future research work, special attention should be paid to the following aspects. Steel structure designers should personally go to the construction site to conduct a comprehensive survey in the early stage of design to ensure that the design work is more scientific and practical; for the inspection of steel material parameters, not only should they master the data indicators such as the width, length, and thickness of the steel material, but also attention should be paid to the plastic properties, strength properties, toughness, etc. of steel structure materials to ensure the stability and safety of steel structure functions; in the process of detailed design, problems or threats in steel structure design should be effectively avoided, such as comprehensive analysis of welding treatment methods and bolt connection method to ensure the feasibility of the connection method.

Data Availability

The experimental data used to support the findings of this study are available from the corresponding author upon request.

Conflicts of Interest

The authors declared that they have no conflicts of interest regarding this work.

References

[1] D. Elwood, A. Schacher, and K. Rhinefrank, "Numerical modeling and ocean testing of a direct-drive wave energy device utilizing a permanent magnet linear generator for power take-off," in *International conference on offshore mechanics and arctic engineering*, vol. 6no. 11, pp. 63–69, Honolulu, Hawaii, USA, 2009.

[2] S. Qiu and H. Wang, "A novel segmented structure and control method for a permanent-magnet linear generator to broaden the range of efficient energy capture," *Journal of*

Marine Science and Engineering, vol. 7, no. 4, pp. 101–112, 2019.

[3] C. Di, "Towering tower steel structure and supporting GRC modular construction technology," *Building Technology Development*, vol. 9, no. 12, pp. 96–100, 2018.

[4] W. Tan, X. Fan, L. Xu, and Y. Wang, "New approach for vibration suppression through restrictors on towering steel columns with supporting frame," *Mathematical Problems in Engineering*, vol. 2020, 16 pages, 2020.

[5] J. P. Gu, Y. X. Qin, Y. Y. Xia et al., "Research on dynamic characteristics of composite towering structure," *International Journal of Applied Mechanics*, vol. 13, no. 8, pp. 78–82, 2021.

[6] L. Aiqun, X. Peng, X. Yiming, and X. Yanhong, "Active vibration control of towering structure and analysis of its installation and commissioning technologies," *Science Discovery*, vol. 4, no. 6, pp. 436–443, 2016.

[7] X. Wang, Y. Xin, and J. Fu, "On comparative analysis of calculation methods for wind loading at towering structure of steel tower mast," *Shanxi Architecture*, vol. 3, no. 11, pp. 99–106, 2015.

[8] Y. Jin and W. C. Yang, "Construction technology of towering structure's verticality control," *Journal of North China institute of Science and Technology*, vol. 11, 2014.

[9] T. Katayama, R. Takano, and T. Yamao, "Experimental study on a performance of seismic vibration control of a cable-mass damper mounted at the top of towering structures," *Journal of Applied Mechanics*, vol. 14, no. 9, pp. 714–725, 2010.

[10] C. G. Jiang, L. U. Guo-Dong, and Y. U. Shao-Feng, "Observation and initial analysis for sunshine deformation of towering reinforced concrete structure," *Beijing Surveying and Mapping*, vol. 9, no. 11, pp. 87–96, 2002.

[11] C. Li, C. Guan, and R. Huang, "The reviews on wind-resistant design of tall buildings and towering structures," *Journal of Guangxi University*, vol. 11, no. 9, pp. 66–72, 1996.

[12] L. J. Liu, F. U. Ye, and B. H. Xiao, "Structure safety identification and analysis of ground type towering billboard," *Construction & Design for Engineering*, vol. 6, no. 10, pp. 110–123, 2016.

[13] A. F. Liu, X. Y. Wu, Z. G. Chen, and W. H. Gui, "An energy-balanced data gathering algorithm for linear wireless sensor networks," *International Journal of Wireless Information Networks*, vol. 17, no. 1-2, pp. 42–53, 2010.

[14] P. E. Kakosimos, E. M. Tsampouris, N. M. Kimoulakis, and A. Kladas, "Overview of the alternative topologies of linear generators in wave energy conversion systems," *Materials Science Forum*, vol. 721, no. 5, pp. 281–286, 2012.

[15] G. Fu and Z. Yu, "Installation method of towering steel pin on some building roof in Sudan," *Construction Technology*, vol. 7, no. 10, pp. 77–82, 2008.

[16] R. Zhigang, L. Peipeng, and W. Qiankun, "Analysis of wind vibration response of TV towers with complex tall steel structures," *Industrial Architecture*, vol. 46, no. 6, pp. 137–143, 2016.

[17] Y. Hui, M. Renle, and H. Minjuan, "Time-history analysis of three-dimensional wind-induced vibration response of complex towering structures," *Special Structures*, vol. 24, no. 4, pp. 45–49, 2007.

[18] L. Zhongxue, D. Changgen, and S. Zuyan, "Nonlinear dynamic buckling and stability analysis of rod steel structures," *China Academic Journal Abstracts (Science and Technology Letters)*, vol. 4, no. 6, pp. 734–736, 1998.

[19] D. Liusheng, S. Mingzhou, F. Zhenggang, and W. Zhe, "Nonlinear finite element analysis of seismic performance of high-strength steel composite K-shaped eccentrically braced steel frame," *Building Structure*, vol. 46, no. 7, pp. 86–92, 2016.

[20] C. Zhaohui, T. Yuchen, and Y. Yongbin, "Elastic-plastic nonlinear analysis method of space frame based on rigid body criterion," *Journal of Building Structures*, vol. 41, no. 10, pp. 139–149, 2020.

[21] C. Xin and W. Huigang, "Review of nonlinear analysis methods for steel frames," *Steel Structure*, vol. 6, no. 31, pp. 1–6, 2016.

[22] Z. Fankui, Z. Junce, W. Jinxin, Y. C. Fan, and C. M. Hu, "Research on direct analysis method of fastener-type steel tube formwork support," *Journal of Xi'an University of Architecture and Technology (Natural Science Edition)*, vol. 53, no. 4, pp. 472–478, 2021.

[23] L. Zhanke, J. Lujun, and Z. Xuhong, "Research status and prospect of direct analysis of overall stability of steel components," *Journal of Building Structures*, vol. 42, no. 8, pp. 1–12, 2021.

[24] W. Xiaolong and Z. Liming, "Application analysis of direct analysis method in the design of double-braced steel derrick structure," *Engineering Construction and Design*, vol. 3, pp. 66–71, 2018.

[25] W. Guping, C. Xuan, and L. Binai, "Application of direct analysis method in structural design of steel structure substation," *Electric Power and Energy*, vol. 42, no. 3, pp. 277–279, 2021.